



Study on nuclear magnetic resonance of superionic conductor NH_4HSeO_4 in rotating frame

Jae Hun Choi¹ and Ae Ran Lim^{1,2,*}

¹Department of Carbon Fusion Engineering, Jeonju University, Jeonju 560-759, Korea

²Department of Science Education, Jeonju University, Jeonju 560-759, Korea

Received April 10, 2014; Revised May 2, 2014; Accepted June 10, 2014

Abstract In order to obtain information on the structural geometry of NH_4HSeO_4 near the phase transition temperature, the spectrum and spin-lattice relaxation time in the rotating frame $T_{1\rho}$ for the ammonium and hydrogen-bond protons were investigated through ^1H MAS NMR. $T_{1\rho}$ for the hydrogen-bond protons abruptly decreased at high temperature and it is associated with the change in the structural geometry in $\text{O}-\text{H}\cdots\text{O}$ bonds. This mobility of the hydrogen-bond protons may be the main reason for the high conductivity.

Keywords: Proton conduction, Hydrogen bonds, Superprotonic conduction, Nuclear magnetic resonance

Introduction

MeHXO_4 (Me: K, Rb, Cs, NH_4 and X: S, Se) materials exhibit fast proton-transport and high electrical conductivity. Hydrogen selenate crystals, HSeO_4^- , are of great interest owing to their complex phase transition sequence and physical properties. Of these, ammonium hydrogen selenate, NH_4HSeO_4 , belongs to the family of hydrogen-bonded crystals with a general formula of MeHXO_4 . This compound undergoes a series of phase transitions with varying temperature. At high temperatures, the crystal attains

a superionic conducting phase, in which the conductivity is due to mobile protons. NH_4HSeO_4 can undergo four phase transitions and the five phases are denoted from I to V in the order of decreasing temperature [1-11]. Below the melting temperature of 427 K ($=T_m$), the crystal is in a high temperature phase (I) and has superionic conductivity. The transition to paraelectric phase (II) occurs at 417 K ($=T_{SI}$), when the crystal is paraelectric monoclinic with space group B2. The crystal then transits to the incommensurate phase (III) at 261 K ($=T_i$) and to the ferroelectric phase (IV) at 250 K ($=T_{C1}$). When the temperature drops below 98 K ($=T_{C2}$), the crystal commences its low temperature phase and becomes non-ferroelectric [12-14].

Previous studies of NH_4HSeO_4 with ^1H nuclear magnetic resonance (NMR) spectra, nuclear spin-spin relaxation times T_2 , in the laboratory frame and conductivity measurements in the vicinity of T_{SI} concluded that the diffusions of protons and NH_4^+ cations in the crystals were isotropic [15,16]. In addition, the microscopic mechanism of deuteron transport in ND_4DSeO_4 crystals was studied by means of ^2H NMR [13, 17-19]. A detailed analysis of the behavior of the ammonium and HSeO_4 deuterons in ND_4DSeO_4 was discussed by Ivanov et al. [13]. Early ^1H NMR investigations of NH_4HSeO_4 only described the average behavior of protons belonging to the hydrogen-bond and NH_4 groups. However, these studies were unable to provide insight into the

* Address correspondence to: Ae Ran Lim, Tel:+82-(0)63-220-2514; Fax: +82-(0)63-220-2053; E-mail: aeranlim@hanmail.net, arlim@jj.ac.kr

microscopic mechanism of the conductivity of the crystals. In our previous report of the NMR and differential scanning calorimetry (DSC) measurements [20], the results indicated a phase transition at 400 K. This was inconsistent with the commonly reported temperature of 417 K [1-11], but agreed with the reports by Czaplá and Moskvich et al. [21, 22]. Recently, Lim et al. [20] studied the roles of ammonium protons and hydrogen-bond protons in the superionic conductor NH_4HSeO_4 by ^1H spin-lattice relaxation time in the laboratory frame T_1 by single-crystal NMR.

The objective of the current study is to understand the mechanism of the phase transitions of NH_4HSeO_4 by characterizing the molecular motions of the NH_4^+ and HSeO_4^- ions with the spin-lattice relaxation time in the rotating frame $T_{1\rho}$ by magic angle spinning (MAS) NMR. The relationship between the dynamical transfer of hydrogen atoms and structural phase transitions is of particular interest. In this paper, the temperature dependences of the intensities, the chemical shifts, and $T_{1\rho}$ for the ^1H nuclei in NH_4HSeO_4 are evaluated in order to elucidate the relationship between the dynamical transfer of hydrogen atoms and the structural phase transitions. Emphasis is placed on the roles of the ammonium and hydrogen-bond protons. These results enable us to compare the phase transition mechanisms and the molecular motions for ammonium protons and hydrogen-bond protons by the MAS NMR.

Crystal structure

The NH_4HSeO_4 crystals in high-temperature phase I has a monoclinic structure with $Z=4$ in unit cell. The unit cell dimensions are $a=7.788 \text{ \AA}$, $b=7.707 \text{ \AA}$, $c=7.924 \text{ \AA}$ and $\gamma=112.51^\circ$ with a symmetry that is close to hexagonal [23]. At room temperature, NH_4HSeO_4 crystals are characterized by a monoclinic structure, and the lattice parameters $a=19.745 \text{ \AA}$, $b=4.611 \text{ \AA}$, $c=7.552 \text{ \AA}$, $\gamma=102.56^\circ$, and $Z=6$. The structure consists of infinite chains of HSeO_4^- anions linked by strong $\text{O-H}\cdots\text{O}$ hydrogen bonds along the b -axis, as shown in Fig. 1 [24, 25]. One-dimensional chains parallel to the b -axis are also linked by NH_4^+ ions, but with much weaker $\text{N-H}\cdots\text{O}$

hydrogen bonds along the a - and c -axes [26, 27]. The symmetry in the ferroelectric phase below 250 K is triclinic with lattice constants $a=10.487 \text{ \AA}$, $b=4.598 \text{ \AA}$, $c=7.507 \text{ \AA}$, $\alpha=90.02^\circ$, $\beta=110.91^\circ$, and $\gamma=101.67^\circ$ [28].

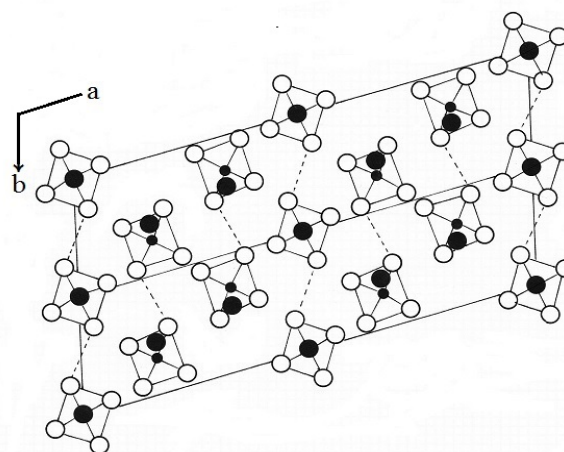


Figure 1. The crystal structure of NH_4HSeO_4 projected onto the ab -plane at room temperature. The dark circles represent NH_4 , medium dark circles Se, open circles O, and dotted lines indicate $\text{O-H}\cdots\text{O}$ hydrogen-bonds.

Experimental method

Single crystals of NH_4HSeO_4 were grown from an aqueous equimolar solution of H_2SeO_4 and $(\text{NH}_4)_2\text{SeO}_4$ by slow evaporation. The crystals were transparent with polygonal plates parallel to the (100) cleavage plane. Occasionally, the crystals exhibited twin structures at room temperature and were slightly hygroscopic.

The ^1H MAS NMR spectrum and the spin-lattice relaxation time in the rotating frame $T_{1\rho}$ were measured by Bruker DSX 400 FT NMR spectrometer at the Korea Basic Science Institute. The Larmor frequency was set at 400 MHz, and the sample powder was placed in a 4 mm CP/MAS probe. The rotor was spun at 10 kHz to minimize spinning sideband overlap. $T_{1\rho}$ was measured by varying the duration of a ^1H spin-locking pulse applied after a direct polarization, i.e., through $\pi/2$ -spinlock acquisition. The $\pi/2$ pulse time for ^1H was 6.67 μs , which was equivalent to a spin-locking field strength of 37.48 kHz. The ^1H $T_{1\rho}$ was measured by applying

^1H spin-locking pulses. The temperature varied from 200 to 425 K in this temperature dependence study. The sample was maintained at a constant temperature through the control of the helium gas flow and the heater current.

Experimental results and analysis

Structural analysis of the protons in NH_4HSeO_4 was carried out by a solid state NMR method. Figure 2 shows the ^1H MAS NMR spectra of NH_4HSeO_4 at several temperatures. NH_4HSeO_4 possesses two kinds of protons; ammonium protons and hydrogen-bond protons. Signals from the ammonium and hydrogen-bond protons overlap, as shown in Fig. 2. The protons in NH_4^+ and HSeO_4^- ions yield two superimposed lines with a ratio of 4:1. The broad and narrow signals in the spectrum for the ammonium and hydrogen-bond protons are obtained by the number of the 4 protons in the NH_4^+ and 1 proton in the HSeO_4^- , respectively. In addition, two peaks at 5.08 and 7.19 ppm are observed in each NMR spectrum, originating from the hydrogen-bond protons and ammonium protons, respectively. Here, the line widths for the two types of protons cannot be distinguished because of the overlap of the two resonance lines.

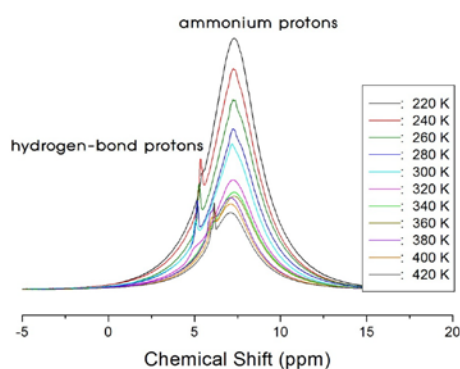


Figure 2. The ^1H MAS NMR spectra of NH_4HSeO_4 at several temperatures.

As the temperature increases, the resonance line area decreases instead of the line widths; the line area is greatly reduced above 320 K. The signal intensities for the ammonium and hydrogen-bond protons are

shown in Fig. 3 as a function of temperature. The intensity for the ammonium protons continuously decreased near T_{Cl} and T_i and abruptly weakened at high temperature T_{Sl} . Conversely, the intensity for the hydrogen-bond protons initially decreased and then increased with increasing temperature, at temperature near T_{Sl} , the intensity increased to be almost equivalent to that of the ammonium protons.

At T_{Sl} , the ordering of the ammonium and hydrogen-bond protons is obvious. The decrease in the intensities of the signals from the two kinds of protons with the increase in temperature is related to the ordering, as previously reported [29].

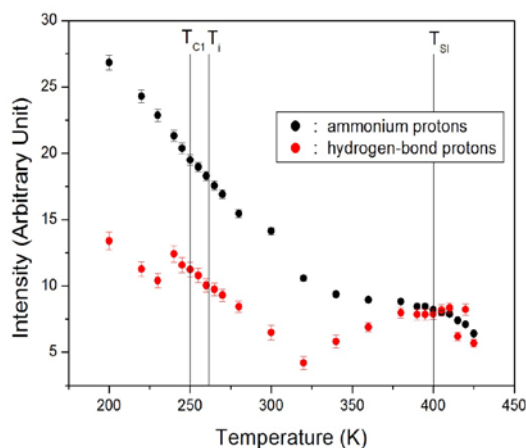


Figure 3. Temperature dependences of the intensities for ammonium protons and hydrogen-bond protons in NH_4HSeO_4 .

Figure 4 shows the chemical shift of the protons with the change in temperature. The chemical shift for ammonium protons remained almost constant with increasing temperature, whereas the chemical shift for hydrogen-bond protons abruptly changed at about 330 K. This abrupt change in the chemical shift near 330 K may be associated with the change in the structural geometry in hydrogen-bond protons, as shown in Fig. 1; the chains of HSeO_4^- anions linked by $\text{O}-\text{H}\cdots\text{O}$ hydrogen bonds change with the increasing temperature; the changes in the chemical shift for hydrogen-bond protons are related to the breaking of an $\text{O}-\text{H}\cdots\text{O}$ bond and the formation of a new H-bond with HSeO_4^- .

The spin-lattice relaxation time in the rotating frame $T_{1\rho}$ for the ammonium and hydrogen-bond protons as

a function of inverse temperature was also studied.

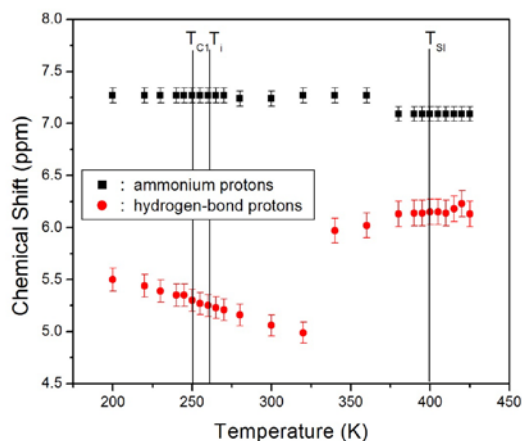


Figure 4. Temperature dependences of the chemical shifts of ammonium protons and hydrogen-bond protons in NH_4HSeO_4 .

$T_{1\rho}$ measurements provide additional information that can be used for more reliable checks on various models of motion. The nuclear magnetization recovery traces obtained for ammonium and hydrogen-bond protons for all temperatures are described by the following single exponential function: $M(t) = M_0 \exp(-t/T_{1\rho})$, where $M(t)$ is the magnetization at time t and M_0 is the total nuclear magnetization of ^1H at thermal equilibrium [30]. The slopes of the recovery trace are different at several temperatures. The temperature dependences of $T_{1\rho}$ for the two kinds of protons are shown in Fig. 5. For both types of protons, $T_{1\rho}$ increased with the temperature, forming a maximum values at around 360 K. The $T_{1\rho}$ of the ammonium and hydrogen-bond protons in NH_4HSeO_4 did not change significantly near the phase transition of T_{C1} , but decreased considerably near the phase transition temperature of T_{Si} . As shown in Fig. 5, near T_i , $T_{1\rho}$ for ammonium protons does not change, whereas that $T_{1\rho}$ for hydrogen-bond protons changes significantly. The phase transition at T_{Si} is of second-order, and above T_{Si} , $T_{1\rho}$ for hydrogen-bond protons is smaller than that for ammonium protons.

In the low-temperature region, the ^1H NMR relaxation time in the rotating frame show a fast-motion limit of the Bloembergen-Purcell-Pound (BPP) [31] type of relaxation as shown in Fig. 5.

Changes in the slopes of the temperature-dependent $T_{1\rho}$ are noticed at around 360 K. Accordingly, the activation energy E_a for ammonium protons obtained from the $T_{1\rho}$ vs. inverse temperature plots changed from 13.22 kJ/mol to 36.52 kJ/mol around 360 K, whereas it for hydrogen-bond protons obtained from the same method plots changed from 12.81 kJ/mol to 50.47 kJ/mol. The E_a for the ammonium and hydrogen-bond protons in the low-temperature is very similar within error range. And, the relaxation time in the high-temperature region was obtained to the slow-motion limit. The change in the E_a of the hydrogen-bond protons at around 360 K may be related to the $\text{O}-\text{H}\cdots\text{O}$ bond near T_{Si} .

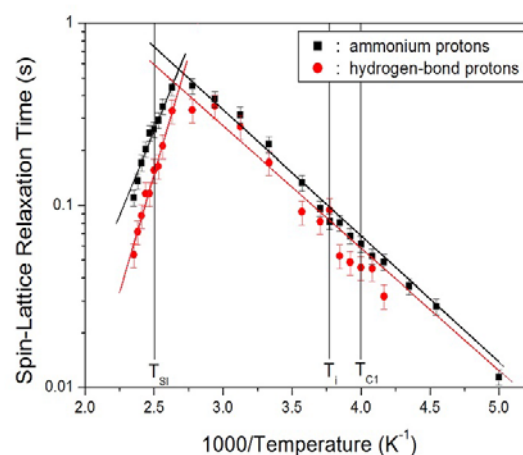


Figure 5. Temperature dependences of the spin-lattice relaxation time in the rotating frame $T_{1\rho}$ for ammonium protons and hydrogen-bond protons in NH_4HSeO_4 .

Discussion and conclusion

In order to obtain the information on the structural geometry near phase transition temperatures, the intensities, chemical shift, and spin-lattice relaxation time in the rotating frame of the ammonium protons and hydrogen-bond protons in NH_4HSeO_4 were investigated by ^1H MAS NMR. The changes in the chemical shifts, the intensities, and $T_{1\rho}$ near the phase transition temperatures were explained by a structural phase transition, indicating that the structural geometry depends on the temperature. The change in the chemical shift for hydrogen-bond protons is associated with the change of structural geometry in

O–H···O bonds. Above T_{SI} , $T_{1\rho}$ for the hydrogen-bond protons abruptly reduced to short values, which corresponds to the breaking of an O–H···O bond and the formation of a new H-bond with HSeO_4^- . This implies that the mobility of the hydrogen-bond protons may be the main reason for

the high conductivity. Consequently, the microscopic environment and dynamics associated with the hydrogen-bond protons in the NH_4HSeO_4 were sensitively reflected in our ^1H NMR $T_{1\rho}$ in rotating frame.

Acknowledgement

This research was supported by the Basic Science Research program through the National Research Foundation of Korea (NRF) funded by the Ministry of Education, Science, and Technology (2012001763).

References

1. Z. Czapla, T. Lis, and L. Sobczyk, *Phys. Status Solidi A* **51**, 609 (1979).
2. A. I. Kruglik, S. V. Misyul, and K. S. Aleksandrov, *Sov. Phys. Dokl.* **25**, 871 (1980).
3. K. Gesi, *J. Phys. Soc. Jpn.* **48**, 1399 (1980).
4. J. Majszczyk, J. Raczka, and Z. Czapla, *Phys. Status Solidi A* **67**, k123 (1981).
5. P. Aleksandrova, O. V. Rosonov, Y. A. Suhovsky, and Y. A. Moskvich, *Phys. Lett.* **2**, 25 (1984).
6. P. Aleksandrova, Y. N. Moskvich, O. V. Rozanov, A. F. Sadreev, I. V. Seryukova, and A. A. Sukhovskiy, *Ferroelectrics* **67**, 63 (1986).
7. Z. Czapla, H. Pykacz, and L. Sobczyk, *Ferroelectrics* **76**, 291 (1987).
8. H. Pykacz, Z. Czapla, and J. Mroz, *Phys. Status Solidi A* **105**, k33 (1988).
9. H. Pykacz, *Ferroelectrics Lett.* **9**, 15 (1988).
10. V. Dvorak, M. Quilichini, N. L. Calve, B. Pasquier, G. Heger, and P. Schweiss, *J. Phys. I (France)* **1**, 1481 (1991).
11. A. V. Kityk, O. G. Vlokh, A. V. Zadorozna, and Z. Czapla, *Ferroelectrics Lett.* **17**, 1 (1994).
12. B. Pasquier, N. L. Calve, A. Rozycki, and A. Novak, *J. Raman Spectrosc.* **21**, 465 (1990).
13. Y. N. Ivanov, J. Totz, D. Michel, G. Klotzche, A. A. Sukhovskiy, and I. P. Aleksandrova, *J. Phys.: Condens. Matter.* **11**, 3751 (1999).
14. B. V. Andriyevskiy, Z. Czapla, S. Dacko, and O. Y. Myshchysyn, *Condens. Matter Phys.* **2**, 685 (1999).
15. I. P. Aleksandrova, O. V. Rozanov, A. A. Sukhovskiy, and Y. N. Moskvich, *Phys. Lett. A* **95**, 339 (1983).
16. Y. N. Moskvich, A. A. Sukhovskii, and O. V. Rozanov, *Sov. Phys. Solid State* **26**, 21 (1984).
17. Y. N. Moskvich, O. V. Rozanov, A. A. Sukhovskiy, and I. P. Aleksandrova, *Ferroelectrics* **63**, 83 (1985).
18. Y. N. Ivanov, A. A. Sukhovskiy, I. P. Aleksandrova, J. Totz, and D. Michel, *Phys. Solid State* **44**, 1077 (2002).
19. Y. N. Ivanov, A. A. Sukhovskiy, I. P. Aleksandrova, and D. Michel, *Appl. Magn. Reson.* **28**, 431 (2005).
20. A. R. Lim, S. W. Jang, and J. H. Chang, *J. Phys. Chem. Solids* **69**, 2360 (2008).
21. Z. Czapla, *Acta Phys. Pol. A* **64**, 47 (1982).
22. Y. N. Moskvich, A. A. Sukhovskii, and O. V. Rozanov, *Fiz. Tverd. Tela* **26**, 381 (1984).
23. A. Onodera, A. Rozycki, and F. Denoyer, *Ferroelectrics Lett.* **9**, 77 (1988).
24. F. Denoyer, A. Rozycki, K. Parlinski, and M. More, *Phys. Rev. B* **39**, 405 (1989).
25. K. S. Aleksandrova, A. I. Kruglik, S. V. Misyul, and M. A. Simonov, *Sov. Phys. Crystallogr.* **25**, 654 (1980).
26. I. P. Aleksandrova, P. Colomban, F. Denoyer, N. L. Calve, A. Novak, B. Pasquier, and A. Rozycki, *Phys.*

- Status Solidi A **114**, 531 (1989).
27. I. P. Aleksandrova, D. Kh Blat, V. I. Zinenko, Y. N. Moskvich, and A. A. Sukhovski, *Izv. Akad. Nauk. SSSR* **51**, 1688 (1987).
 28. A. Rozycki, F. Denoyer, and A. Novak, *J. Phys.* **48**, 1553 (1987).
 29. O. V. Rozanov, Yu. N. Moskvich, and A. A. Sukhovskii, *Sov. Phys. Solid State* **25**, 212 (1983).
 30. E. Fukushima and S. B. W. Roeder, *Experimental Pulse NMR*, Addison-Wesley Pub. Company, Massachusetts, (1981).
 31. N. Bloembergen, E. M. Purcell, and R. V. Pound, *Phys. Rev.* **73**, 679 (1948)